Low Temperature Plasma Technology Laboratory

Design of a helicon plasma injector using the HELIC code

Francis F. Chen

Electrical Engineering Department

LTP-202   February, 2002

LTPTL

Electrical Engineering Department
Los Angeles, CA 90095-1594

UNIVERSITY OF CALIFORNIA • LOS ANGELES

Design of a helicon plasma injector using the HELIC code

We start with a 10 cm diam glass tube ~20 cm long, with a 12 cm diam single-loop (multi-turn) antenna 10 cm from the closed end of the tube. A conducting shield is assumed 30 cm from the axis. The B-field is uniform at 150G, and the density is almost flat, with a rolloff at the edge and a central density of 10^{13} cm^{-3}. The argon pressure is 10mTorr, and KT_e is 4eV. The plasma loading R (in ohms) is computed for various variations on these initial parameters.

Standard conditions

a = 5 cm, b = 6 cm, c = 15 cm

$B_0 = 150$G
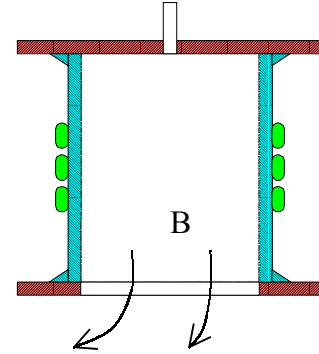
$n_0 = 10^{13}$ cm^{-3}

$p_0 = 10$ mTorr Ar

$KT_e = 4$ eV

Density profile: $n(r) = n_0 [1 - (r/w)^s]^t$, with $s = 10$, $t = 1$, $f_a = .25$ (fraction at $r = a$; this sets w)

The tube is assumed to be 2m long, with insulating boundaries at each end. Thus, injection into a flaring field is neglected; it cannot be handled by HELIC. The parameters are chosen to correspond to a port on the LAPD machine.
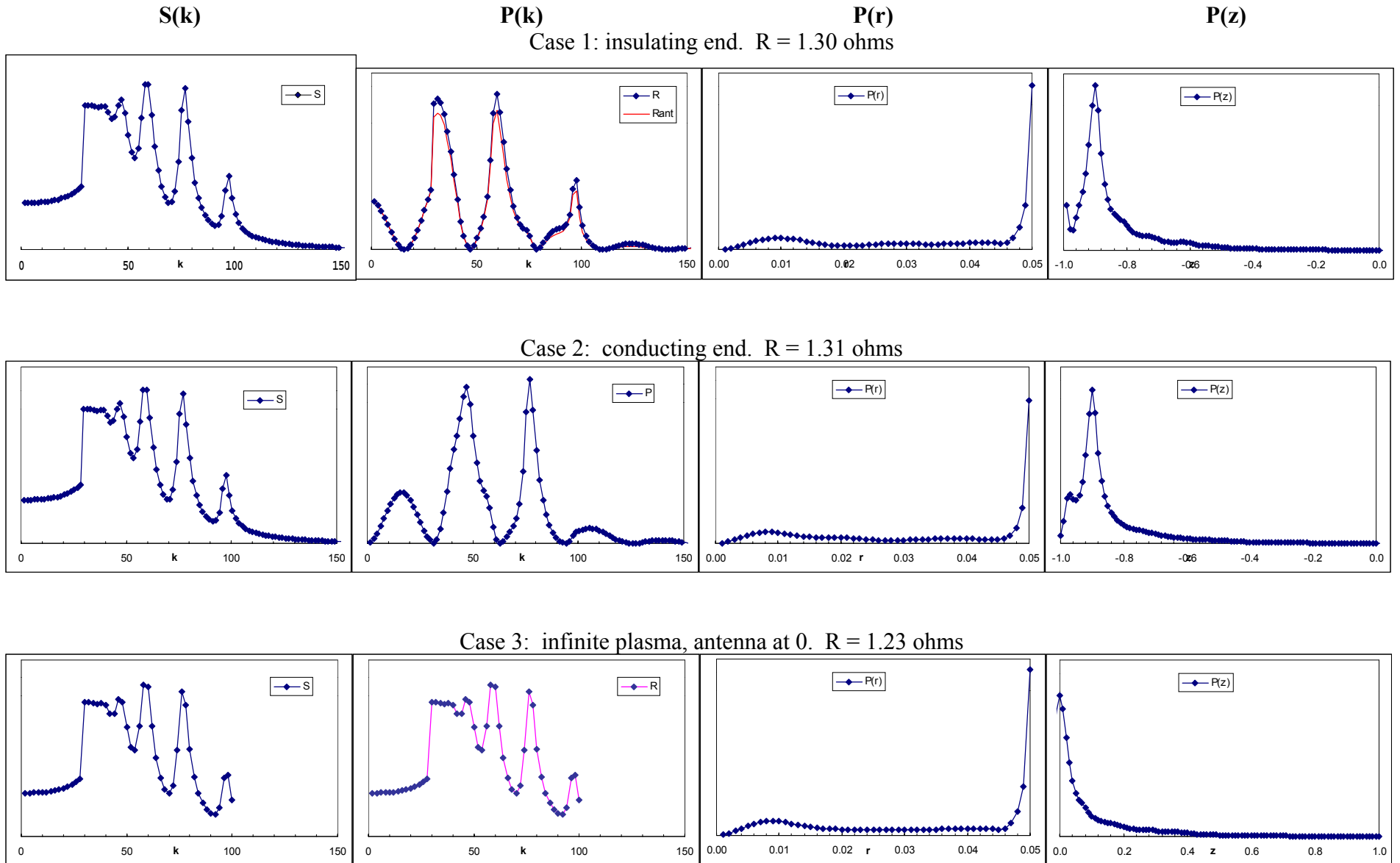
Definitions

In the following graphs, S(k) is the plasma response to various k (in m^{-1}); P(k) is the antenna loading per unit k; P(z) is the loading per unit z, integrated over cross section; and P(r) is $2\pi \times$ the loading per unit r, integrated from z_{min} to z_{max}. Thus, the P(r) curves have to be weighted by r to get a realistic view of the power deposition profile. Here $z_{min} = -1$m and $z_{max} = +1$m, and the antenna midplane is at $d - 1$ m. S(k) depends on the tube size and is independent of the antenna

### Fig. 1: Variation of R with antenna position
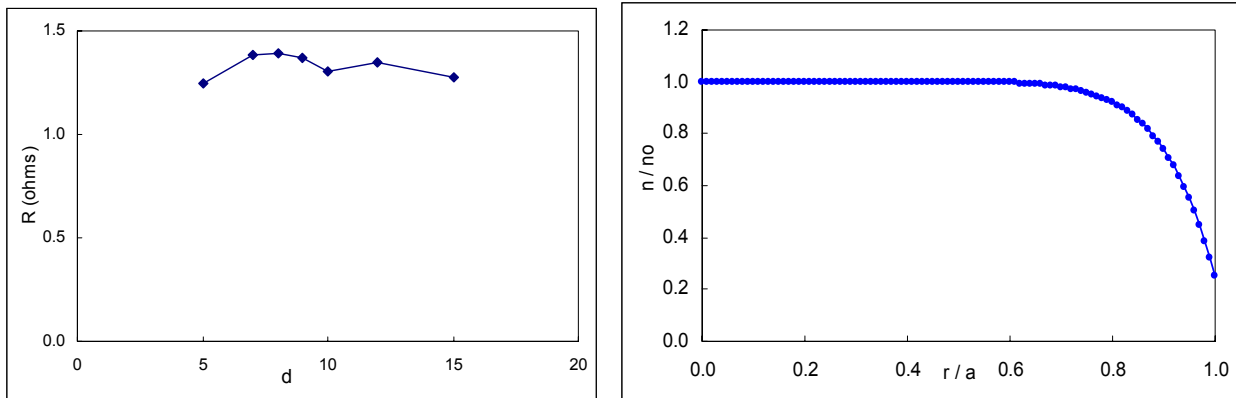
Here d is the distance in cm of the antenna from the closed end of the tube. There is an optimum position, but the variation is small. The (10,1) density profile is at the right.

Fig. 2. Test of boundary conditions

S(k)	P(k)	P(r)	P(z)

Case 1: insulating end. R = 1.30 ohms

Case 2: conducting end. R = 1.31 ohms

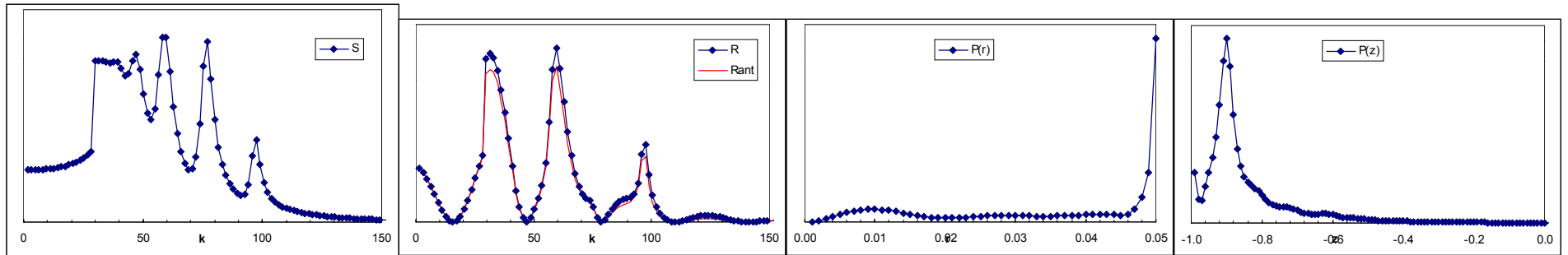Case 3: infinite plasma, antenna at 0. R = 1.23 ohms

Conclusion: Plasma spectrum is same; antenna spectrum is shifted. Loading is insensitive to the boundary condition.

Fig. 3 Test of antenna position
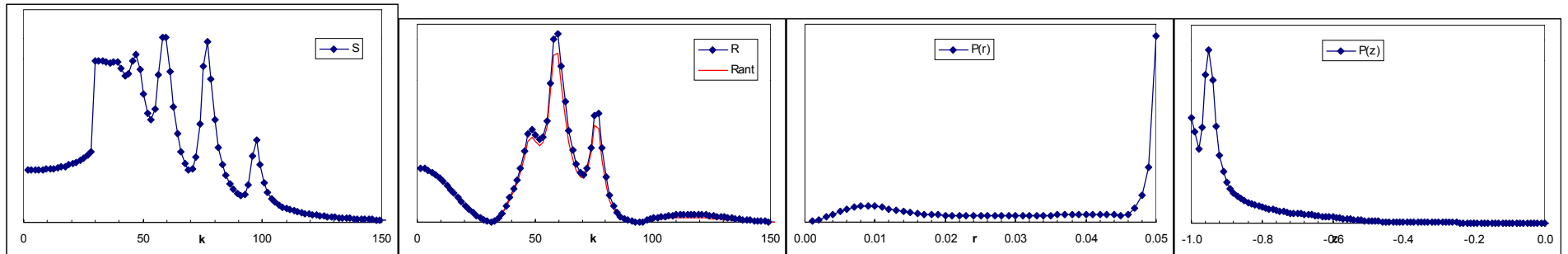
S(k)	**P(k)**	**P(r)**	**P(z)**

Case 5: 15cm from end. R = 1.27 ohms
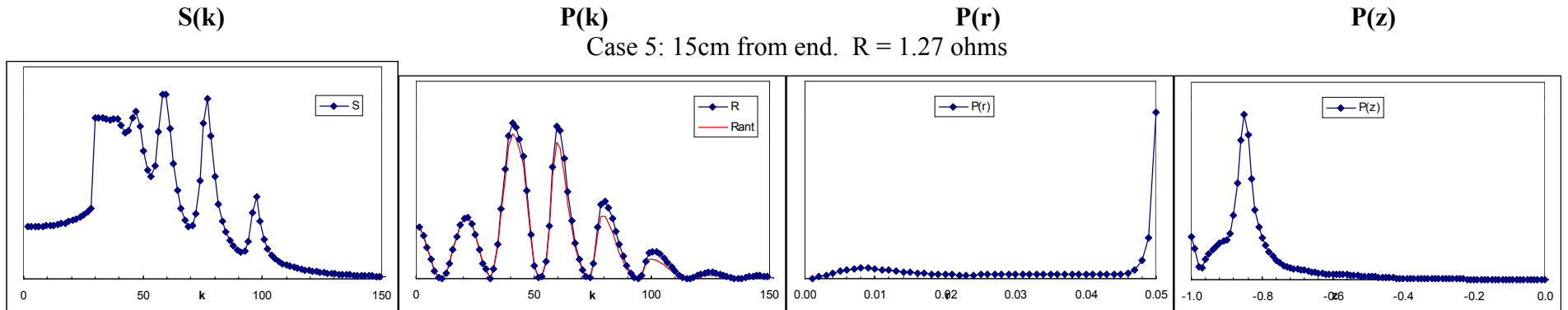
Case 1: 10 cm from end. R = 1.30 ohms
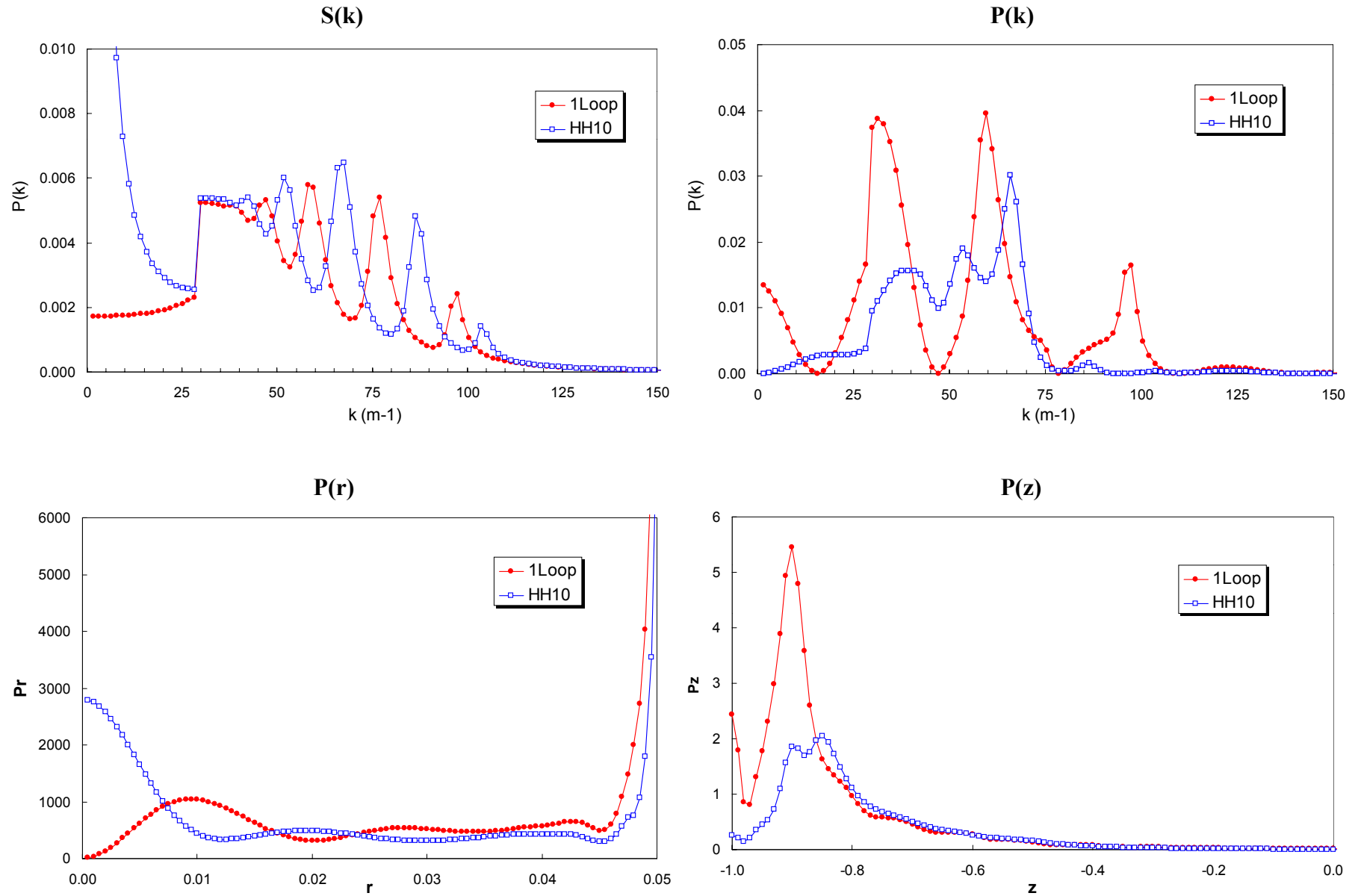

Case 4: 5 cm from end. R = 1.25 ohms

Conclusion: Loading in *z* follows antenna. No. of beats increases with *d*. Radial profile and *R* are insensitive to this.

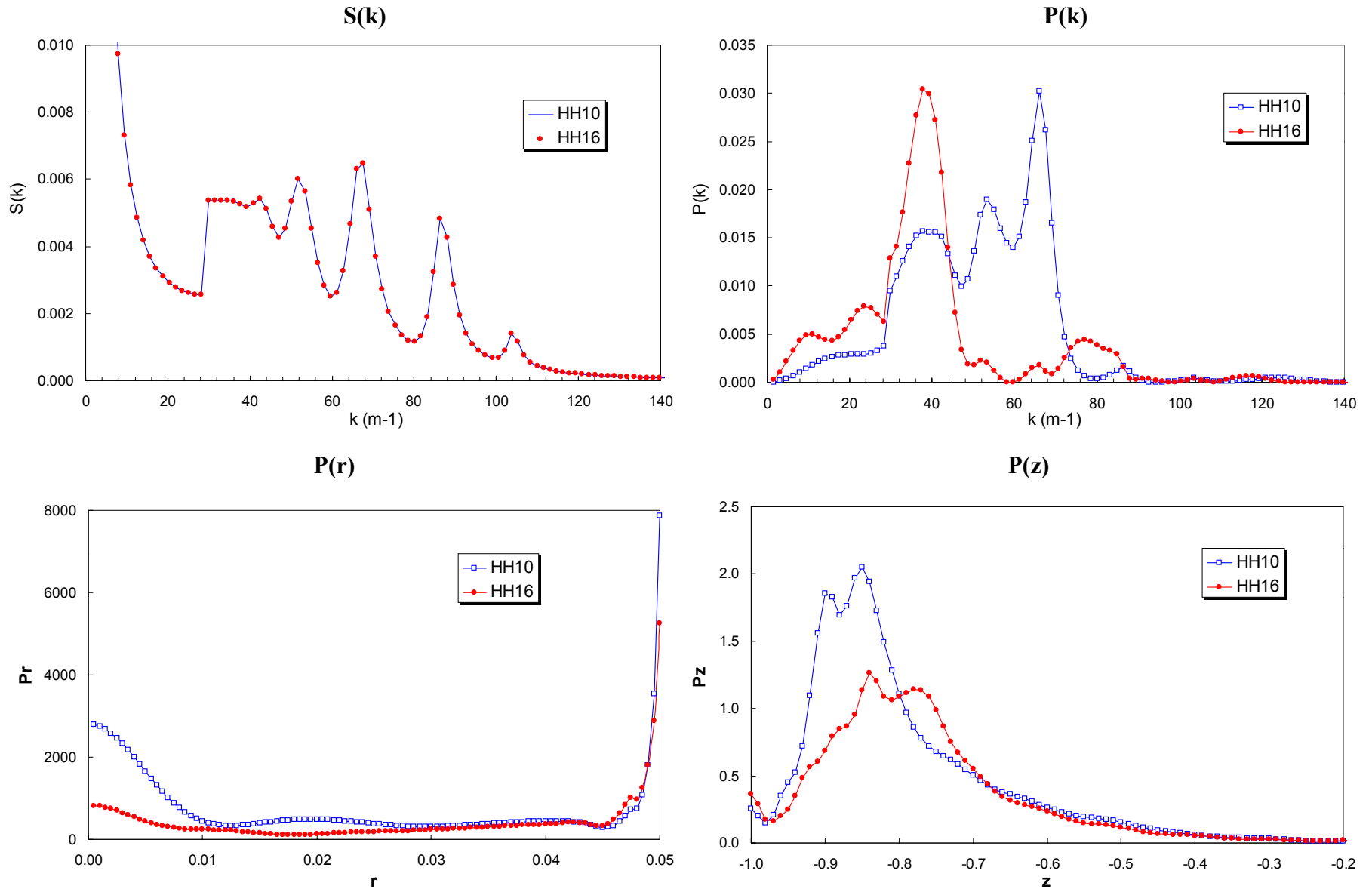**Fig. 4. Compare *m* = 1 (half-helical) and *m* = 0 (single-loop) antennas**

Helical antenna is 10 cm long, centered at *d* = 10 cm   **R = 0.767Ω (HH), 1.228Ω (1L)**

The discontinuity in S(k) is numerical, not real. Conclusion: *m* = 0 couples better, but advantage is at edge.
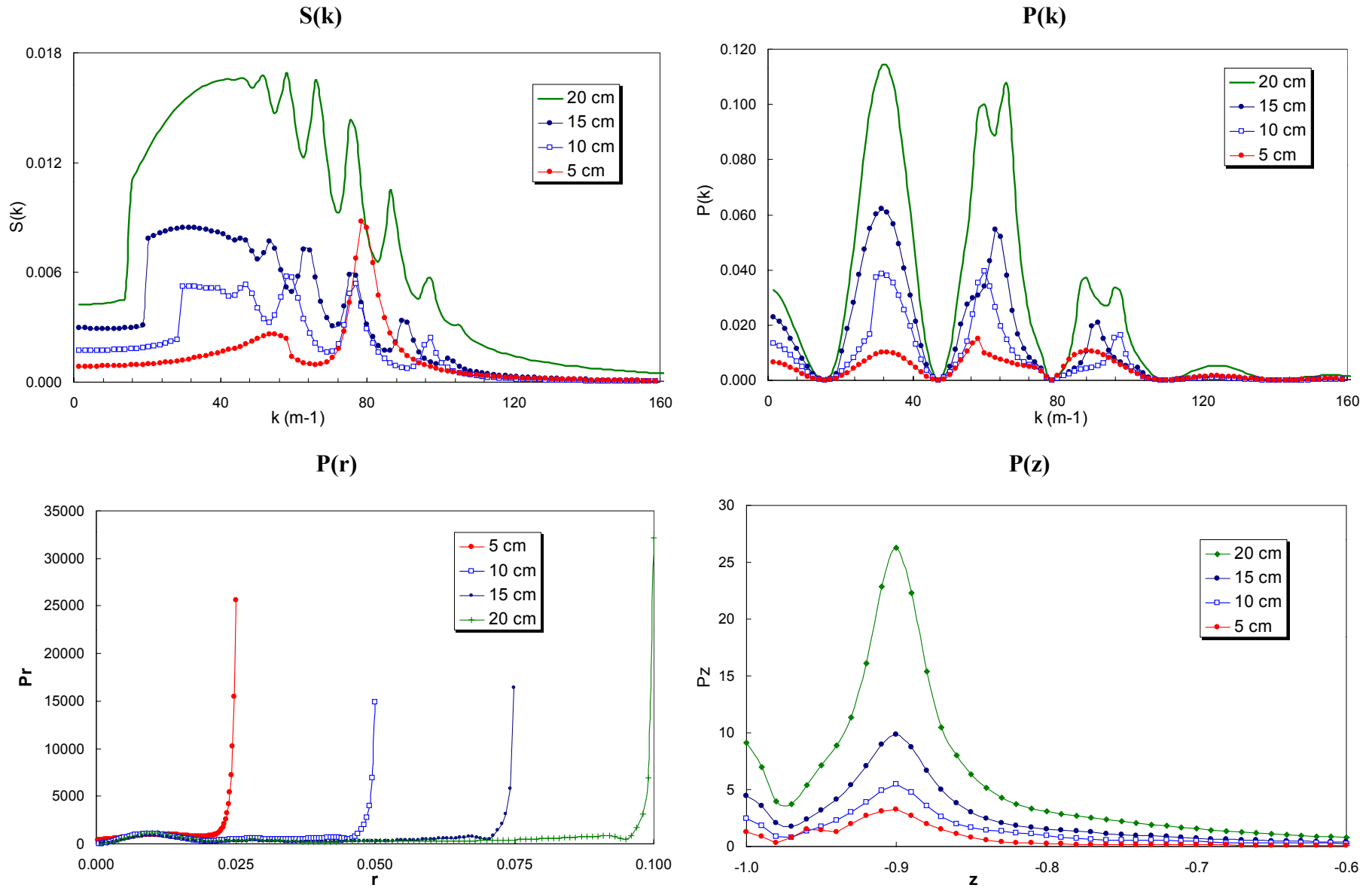
Fig. 5. Compare 10-cm helix (HH10) with 16-cm helix (HH16)

16-cm helix is centered 16cm from end. **R = 0.767Ω (HH10), 0.591Ω (HH16)**
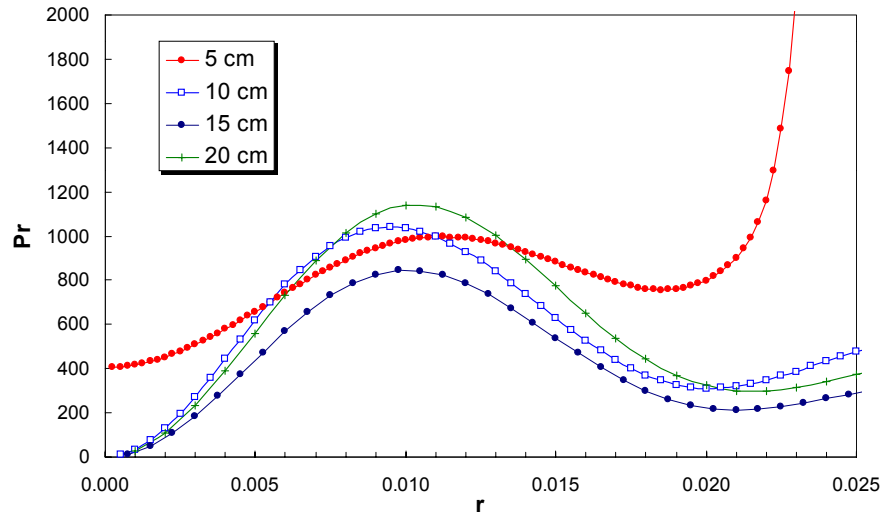
S(k) is the same, of course. Conclusion: The 10 cm length is a better match at this *n* and *B*.

# Fig. 6. Compare tube diameters with a single loop antenna at d = 10 cm

Conclusion: Many more radial modes possible with large radii. Main plasma peaks show up in P(k), since this antenna has a flat spectrum.

Fig. 7. Central portion of P(r) for different tube diameters

Conclusion: The H-mode absorption is about the same for all diameters.

**Fig. 8. Increase in absorption with tube diameter**
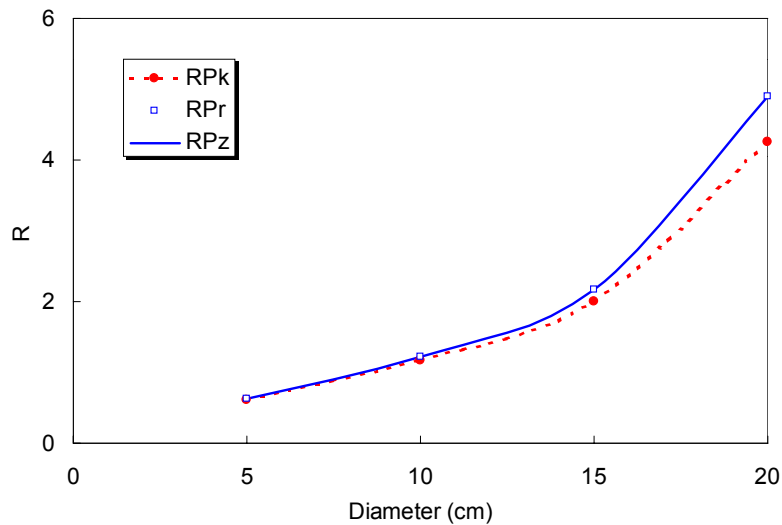
Conclusion: Much better power deposition with large tubes, probably because of the larger volume of plasma and the increase in number of radial modes possible. The curves here differ at large radii because the number of radial steps needed to resolve the TG layer increases, and this affects some calculations more than others.

Fig. 9. Dependence of loading on B-field

(a) at low densities (10^{12} cm^{-3} − 10^{13} cm^{-3})
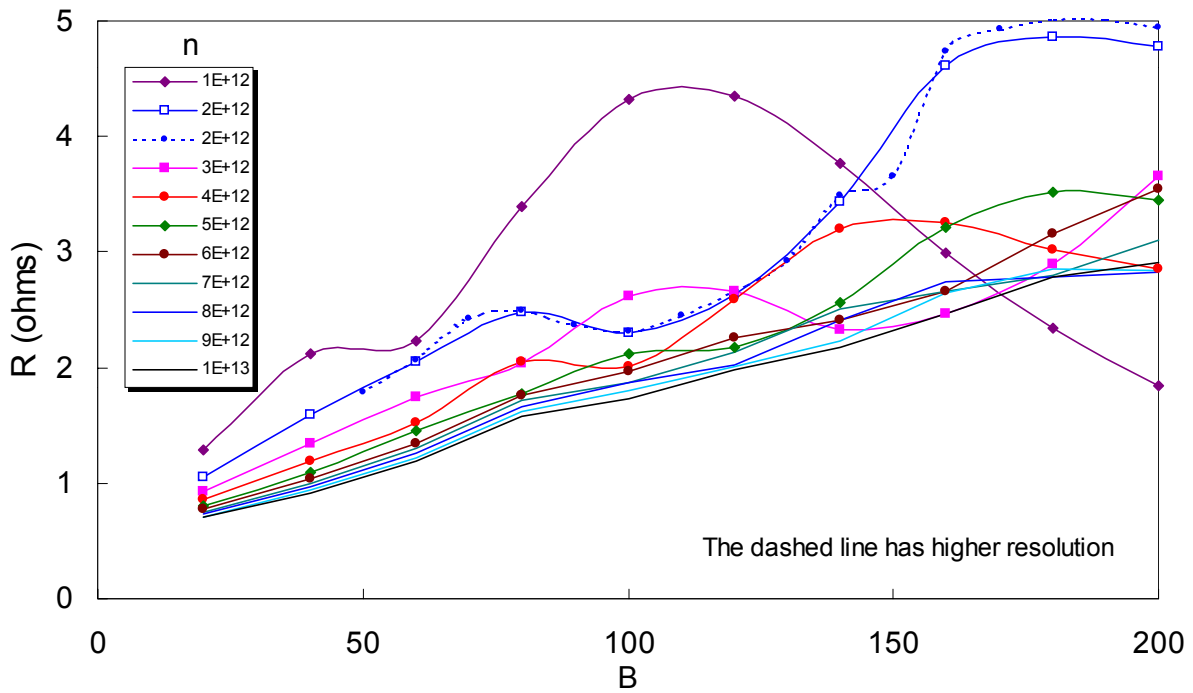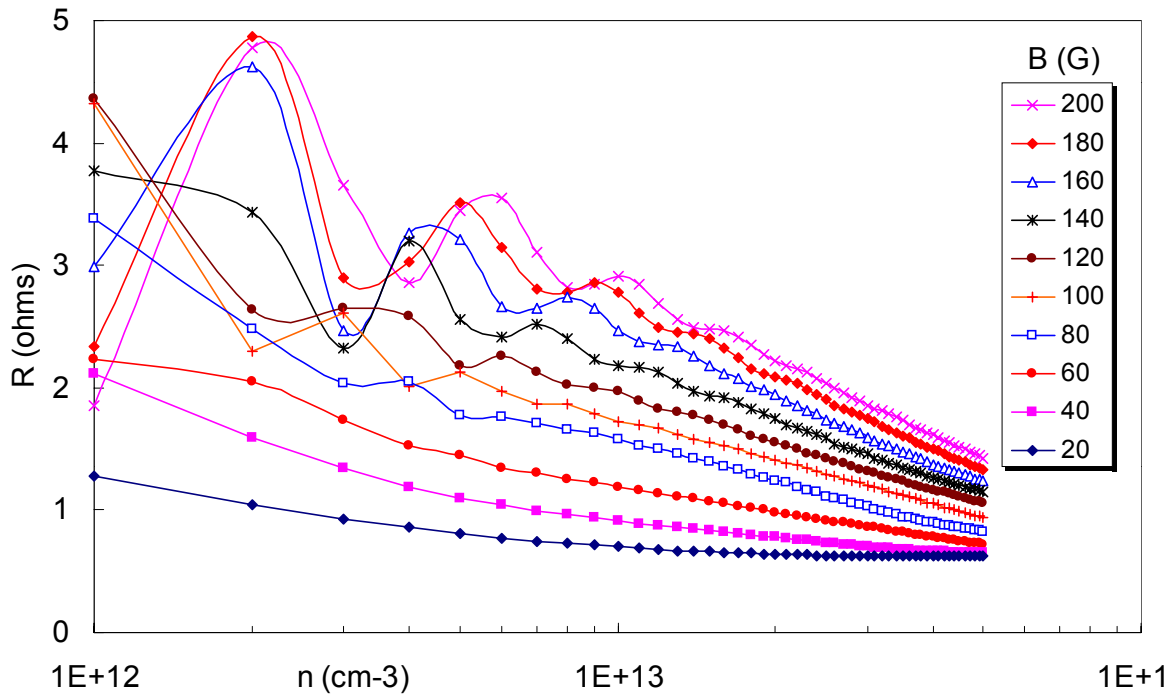

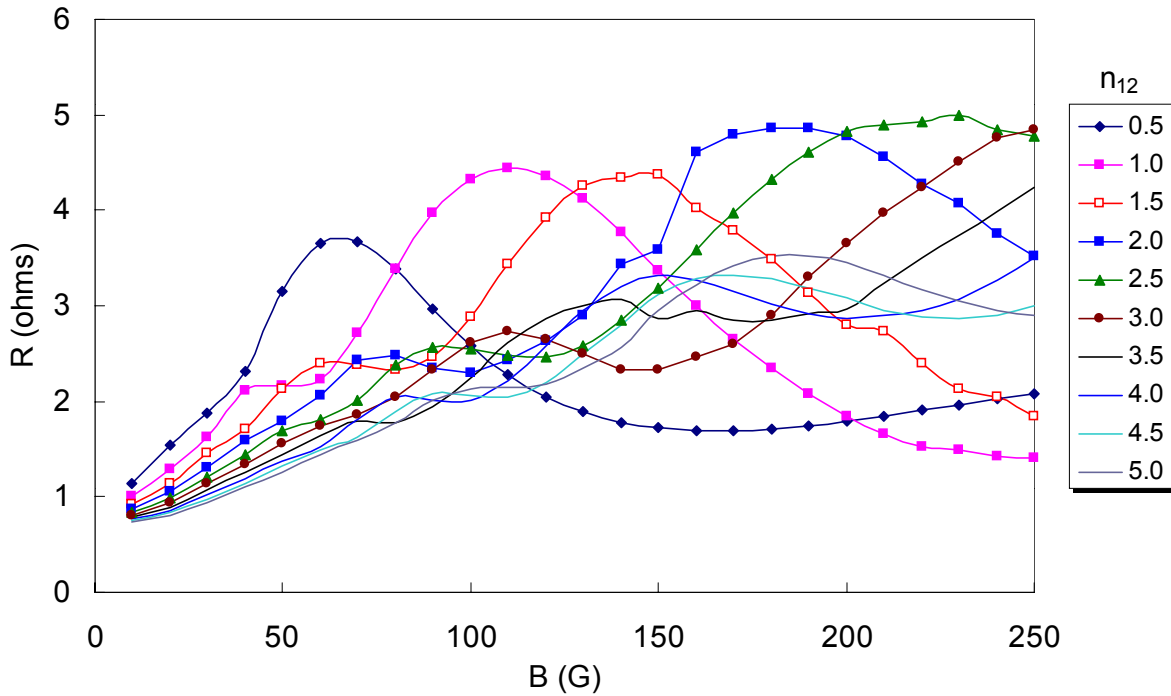(b) at high densities (5×10^{12} cm^{-3} − 5×10^{13} cm^{-3})
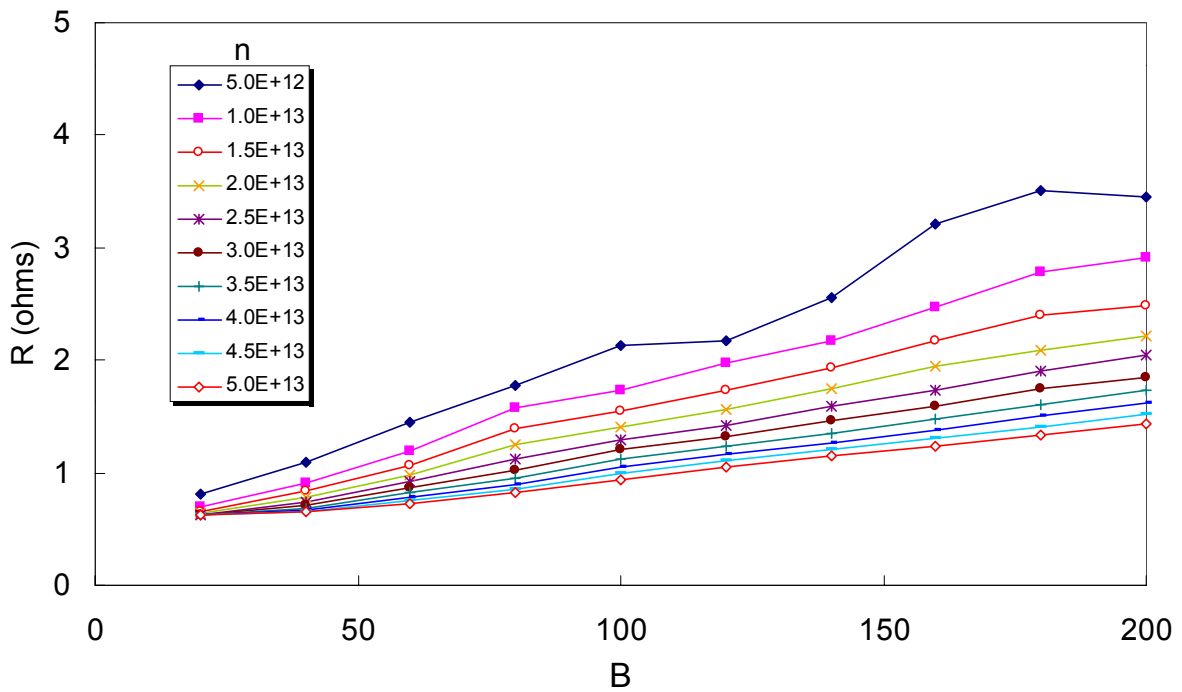
Conclusion: A low-field peak is seen at low densities. At high densities, *R* increases linearly with B.

Fig. 10. Dependence of loading on density

Conclusion: There are large resonances at low *n* and high *B*, but generally *R* decreases with increasing *n*.
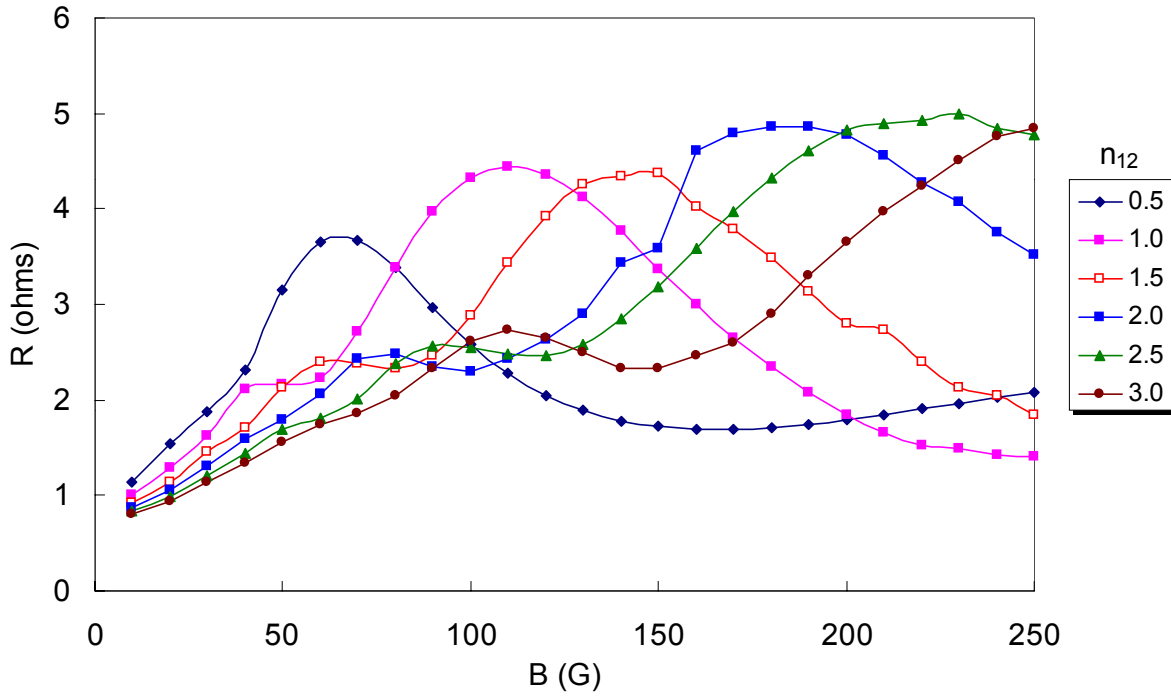
Fig. 11. Investigation of the low-field peak
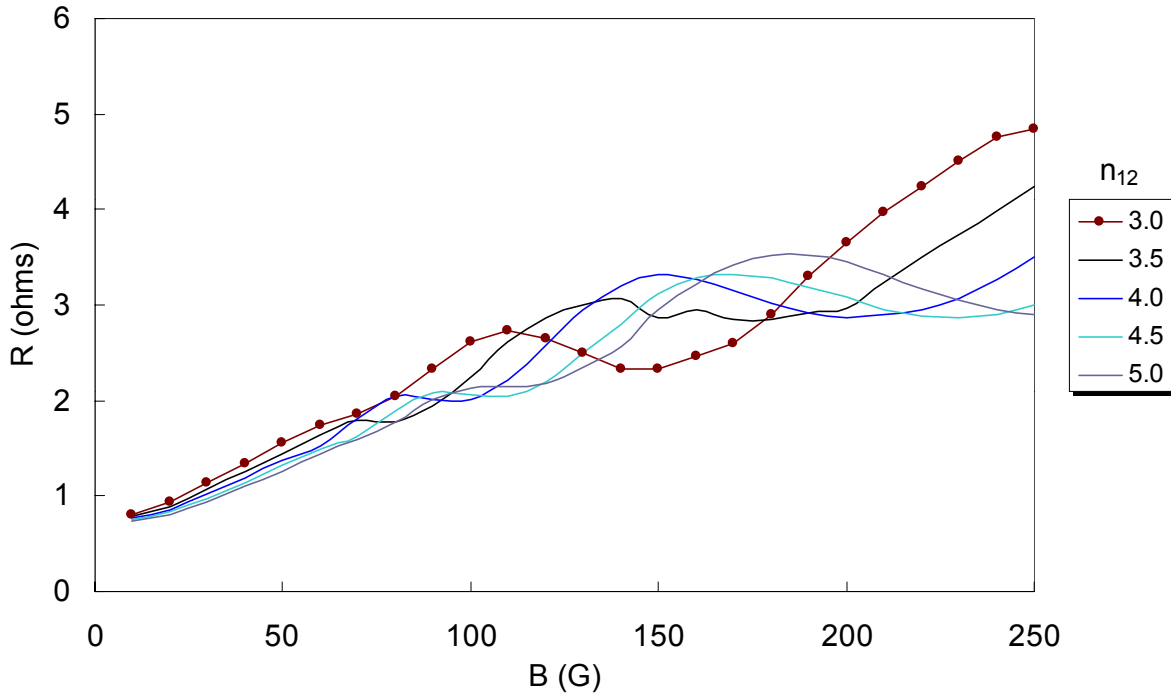

The graph is too busy. It is split below.

Fig. 12. The low-B peak at high and low *n*

(a) $n = 0.5 - 3 \times 10^{12}$ cm^{-3}

(b) $n = 3 - 5 \times 10^{12}$ cm^{-3}

Conclusion: The peak shifts to higher *B* as *n* increases. Above 3×10^{12} cm^{-3}, a second, smaller peak appears in the original position, and that shifts similarly with *n*. These peaks clearly are not related to the lower hybrid resonance (which is near 1450G) and may be connected to reflections from the endplate or to TG-helicon resonances.

Note that a peak in $R(B)$ at constant n is not the same as a peak in $n(B)$. At B_{peak}, the power deposition increases, so n increases. This moves the plasma to a different n curve. The situation is clearer on Fig. 10, which gives R at constant B. Each curve has stable points on its right and unstable points on its left. The equilibrium n depends on P_{rf}. Thus, there should be a jump in n up to the peak as P_{rf} is increased. It is seen that R has a large maximum in the 160-200G range, but only for densities in the low 10^{12}s.

We next investigate what the low-B peak depends on. First, we sharpen the peak by reducing the pressure to 2 mTorr. In Fig. 13 for $n = 10^{12}$ cm^{-3} we see that the effect is weak, and it is not necessary to reduce p_0 further.

Fig. 13
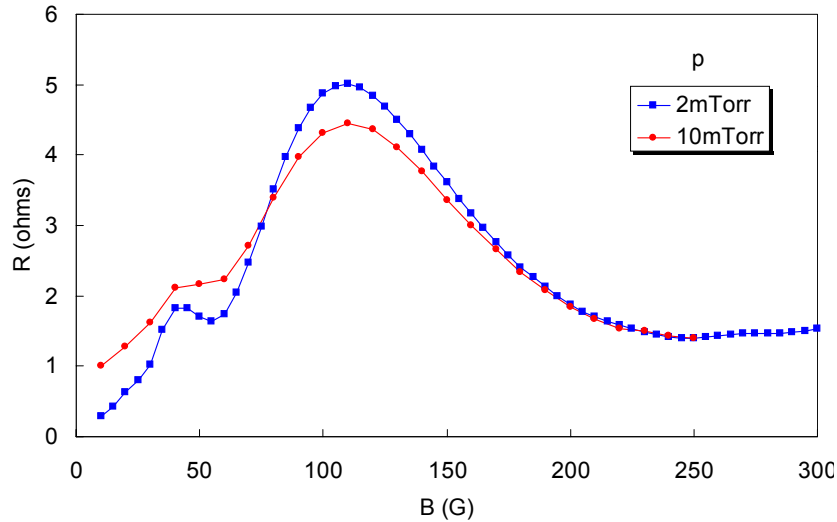
Next, we study the dependence of $R(B)$ on the density profile $n(r)$. Fig. 14 shows the 1×10^{12} cm^{-3} peak for a uniform plasma, a fairly flat plasma with a 75% dropoff at the edge (s = 10, t = 1, fa = 0.25), and a parabolic profile (s = 2, t = 1, fa = 0.1). We see that the profile makes a big difference, suggesting that the helicon-TG mode structure is involved in this resonance. Also, B_{peak} shifts downwards to the range seen in experiments as the profile becomes narrow.

Fig. 14
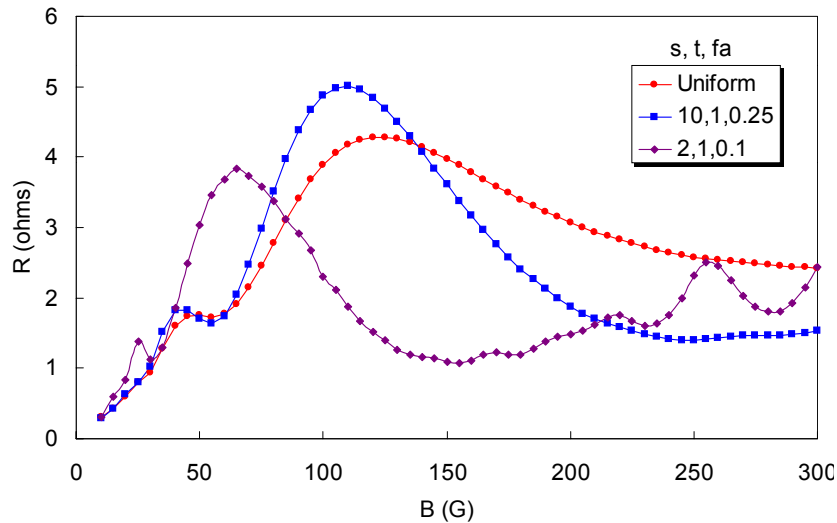
To see if the low-B peak is related to interference with the wave reflected from the endplate, we compute R for the single loop with d = 5 and 10 cm, and with no end boundary. Figure 15 shows that the peak shifts greatly as the distance from the endplate is changed. It disappears altogether in an infinite plasma. Therefore, the low-B peak is almost certainly caused by endplate reflections. The small peaks in the No-Boundary curve may be TG resonances.

Fig. 15
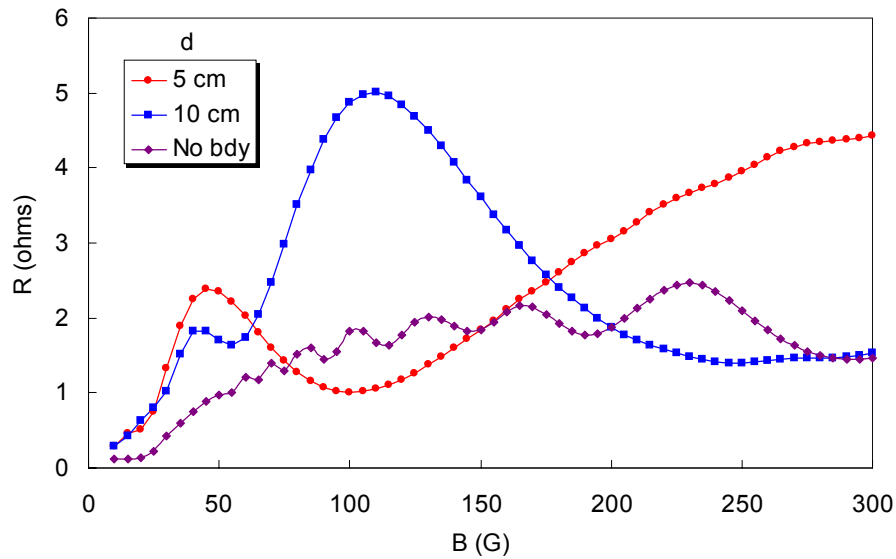
To see the difference in endplate reflections, we next compare a conducting endplate with an insulating one. Figure 16 shows that the boundary condition makes a great difference, supporting the guess that end reflections are the cause of the low-B peak.

Fig. 16
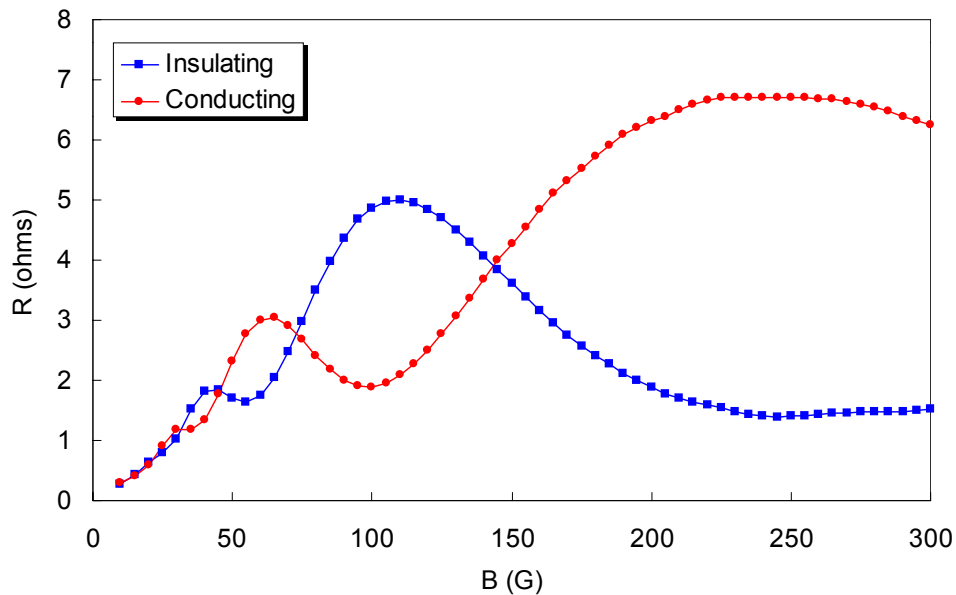
The half-helical antenna launches $m = +1$ waves preferentially downstream, so it is not unexpected that there should be only weak reinforcement of the wave from reflections of the $m = -1$ component. To study this, we next compare antennas for the 10^{12} cm^{-3}, 2mTorr case.

Figure 17 shows $R(B)$ in the low-B peak region for the standard $m = 0$ loop 10 cm from the endplate, for a 10-cm half-helical $m = +1$ antenna centered at d = 10 cm (end ring 5 cm from endplate), and for a 10-cm Nagoya III antenna in the same position. Since the NIII antenna launches $m = +1$ waves in both directions, we would have expected it to generate a large low-B peak. We see that this is not the case. The $m = 1$ antennas have their excitation distributed over a 10 cm length, so the reflections do not constructively interfere at any place. In early experiments in which the low-B peak was detected, its differing height was attributed to a change in tube diameter. Instead, it might have been a change from NIII to HH antennas.

Fig. 17
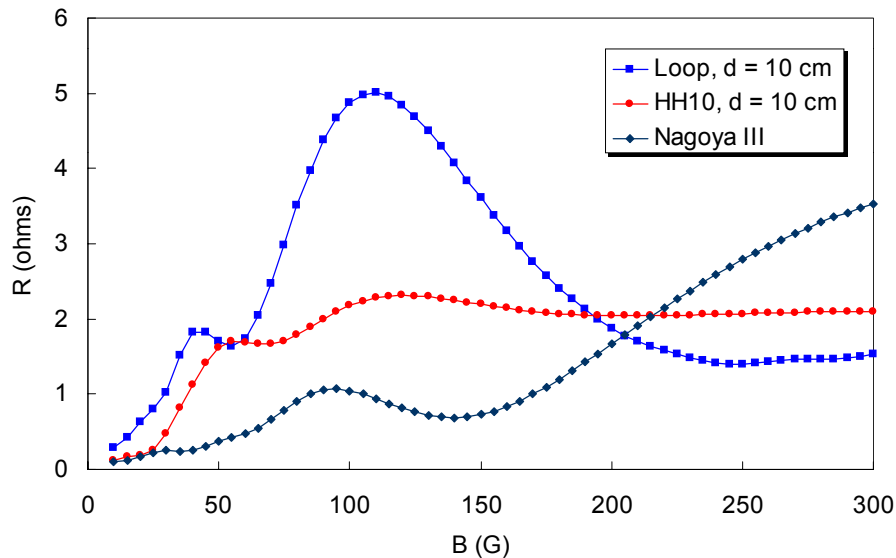
Conclusions

At low B-fields, the single-loop antenna in a stubby tube achieves a loading resistance of order 5 ohms, well above what is usually found for helicon discharges at these fields. This is because its geometry permits strong constructive interference from the wave reflected from the end of the tube. The field at which the peak occurs depends on density, density profile, and the conductivity of the endplate. Once these are fixed, however, B_{peak} can be adjusted by changing the distance d of the loop from the endplate. Unfortunately, this effect disappears at high densities.

Secondly, the antenna loading increases rapidly with tube diameter, and 5-ohm resistances can be obtained even at high density if the diameter is increased to 20cm. This is in spite of the fact that the TG absorption occurs in a very thin layer compared with the radius, and the fall-off of n near the edge has been accounted for in these calculations.